

# Epsilon Sodium Disilicate: A High-Pressure Layer Structure [Na<sub>2</sub>Si<sub>2</sub>O<sub>5</sub>]

Michael E. Fleet

*Department of Earth Sciences, University of Western Ontario, London, Ontario N6A 5B7, Canada*

and

Grant S. Henderson

*Department of Geology, University of Toronto, Toronto, Ontario M5S 3B1, Canada*

Received March 20, 1995; in revised form June 8, 1995; accepted June 12, 1995

Epsilon sodium disilicate ( $\epsilon$ -Na<sub>2</sub>Si<sub>2</sub>O<sub>5</sub>) synthesized at 7 GPa, 1100°C, for a 12-hr run time (M6/8 superpress, Edmonton) is orthorhombic with  $a = 5.580(1)$ ,  $b = 9.441(4)$ ,  $c = 8.356(3)$  Å,  $Pbc2_1$ ,  $Z = 4$ ,  $D_x = 2.749$  g·cm<sup>-3</sup>. The structure ( $R = 4.0\%$ ) is based on a disilicate sheet of alternating six-membered rings of UUUDD and DDDU SiO<sub>4</sub> tetrahedra in the (100) plane, with linking Na(1) five-fold coordinated to 2.57 Å and Na(2) four-fold coordinated to 2.55 Å: (Si(1)—O) = 1.633 Å, Si(1)—O<sub>nbr</sub> = 1.580 Å; (Si(2)—O) = 1.623 Å, Si(2)—O<sub>nbr</sub> = 1.571 Å. The structure is similar to that of  $\beta$ -Na<sub>2</sub>Si<sub>2</sub>O<sub>5</sub>, the 1 bar, 610–700°C polymorph, that has rings of UDUDUD tetrahedra. Densification is accommodated largely by a decrease in dihedral (Si—O—Si) bond angles that range from 127.0 to 129.3°, compared with 135.1° to 137.1° for  $\beta$ -Na<sub>2</sub>Si<sub>2</sub>O<sub>5</sub> ( $D_x = 2.57$  g·cm<sup>-3</sup>) and 138.9° to 160.0° for  $\alpha$ -Na<sub>2</sub>Si<sub>2</sub>O<sub>5</sub> ( $D_x = 2.50$  g·cm<sup>-3</sup>). The  $\epsilon$  phase structure is consistent with <sup>29</sup>Si MAS-NMR and Raman spectra, and supports our earlier suggestion that densification of silicate melts to moderate pressures is accommodated predominantly by a decrease in dihedral bond angle through crimping of ring structures and a decrease in the number of SiO<sub>4</sub> tetrahedra per ring. © 1995 Academic Press, Inc.

## INTRODUCTION

Several of the various room-pressure structural modifications of sodium disilicate (Na<sub>2</sub>Si<sub>2</sub>O<sub>5</sub> (1)) have structures based on sheets of six-membered rings of SiO<sub>4</sub> tetrahedra (e.g.,  $\alpha$ -Na<sub>2</sub>Si<sub>2</sub>O<sub>5</sub> (2);  $\beta$ -Na<sub>2</sub>Si<sub>2</sub>O<sub>5</sub> (3, 4)). Indeed, all known monovalent cation disilicate structures are based on [Si<sub>2</sub>O<sub>5</sub>] disilicate sheets. Following Liebau (5), the structural complexity of layered structure M<sub>2</sub><sup>+</sup>[Si<sub>2</sub>O<sub>5</sub>] phases arises from accommodation of the interlayer monovalent cation, and this is largely determined by cation size. The small cation structures (phyllosilic acid, H<sub>2</sub>Si<sub>2</sub>O<sub>5</sub>, and Li<sub>2</sub>Si<sub>2</sub>O<sub>5</sub>) have very strongly folded (crenulated) disilicate sheets. In  $\alpha$ -

Na<sub>2</sub>Si<sub>2</sub>O<sub>5</sub> (present above 700°C) the disilicate sheets are slightly less folded, and in  $\beta$ -Na<sub>2</sub>Si<sub>2</sub>O<sub>5</sub> (present at 610–700°C) they are markedly less folded. The ideal radius to stabilize a flat disilicate sheet is estimated to be about 1.7 Å, close to the size of the Cs<sup>+</sup> cation. However, the structure of Cs<sub>2</sub>Si<sub>2</sub>O<sub>5</sub> has not been determined, and Liebau (5) suggests that a framework structure would be energetically more favorable anyway.

The crystal chemistry of high-pressure silicate phases contributes to our understanding of the mineralogy and physics of the Earth's interior, and provides insight into the stereochemistry of sixfold coordinated Si and the mechanisms of densification of high-pressure silicate melts (e.g., 5–11).

High-pressure phase relations in the Na<sub>2</sub>O—SiO<sub>2</sub> system were investigated by Kanzaki *et al.* (12); the crystalline phases they reported were  $\epsilon$ -Na<sub>2</sub>Si<sub>2</sub>O<sub>5</sub> at moderate pressure and Na<sub>2</sub>Si<sub>3</sub>O<sub>7</sub>, Na<sub>2</sub>Si<sub>4</sub>O<sub>9</sub>, and stishovite (SiO<sub>2</sub>) at high pressure. Santarsiero *et al.* (13) reported a second high-pressure disilicate phase ( $\zeta$ -Na<sub>2</sub>Si<sub>2</sub>O<sub>5</sub>) and with a partial structure containing [<sup>6</sup>Si:<sup>4</sup>Si] in the ratio 1:6. The present investigation arose from the need for more information on the structures of these crystalline sodium silicates to complement X-ray absorption study (XAS) of high-pressure vitreous products in the Na<sub>2</sub>O—SiO<sub>2</sub> and K<sub>2</sub>O—SiO<sub>2</sub> systems (14; work in progress). We have shown recently (15) that Na<sub>2</sub>Si<sub>3</sub>O<sub>7</sub> has a high-pressure framework structure with silicon in both tetrahedral and octahedral coordination ([<sup>6</sup>Si]:[<sup>4</sup>Si] = 1:2). Preliminary work on the structure of  $\epsilon$ -Na<sub>2</sub>Si<sub>2</sub>O<sub>5</sub> was reported in Ref. (8).

## EXPERIMENTAL PROCEDURES

Epsilon sodium disilicate ( $\epsilon$ -Na<sub>2</sub>Si<sub>2</sub>O<sub>5</sub>) was synthesized using the MA6/8 superpress at the University of Alberta,

Edmonton at 7 GPa, 1100°C, for a 12.3 hr run time (experiment 1919). The charge consisted of glass of bulk composition Na<sub>2</sub>Si<sub>2</sub>O<sub>5</sub> that was placed in a sealed Pt capsule and dried at about 400°C for 2–3 hr before welding. The pressure assembly (without the sample capsule) was fired at 1000°C under a N<sub>2</sub>–H<sub>2</sub> gas mixture for 1 hr. The products consisted of crystals of ε-Na<sub>2</sub>Si<sub>2</sub>O<sub>5</sub> (up to 0.15 mm in diameter) together with minor amounts of crystals of wadeite-structure Na<sub>2</sub>Si<sub>4</sub>O<sub>9</sub>. In refractive index oil, ε-Na<sub>2</sub>Si<sub>2</sub>O<sub>5</sub> is colorless, markedly anisotropic with perfect {100} cleavage and weak birefringence normal to the *a*-axis and strong birefringence in orientations parallel to the *a*-axis, and biaxial negative ( $2V \approx 40\text{--}45^\circ$ ). The composition of the crystals of ε-Na<sub>2</sub>Si<sub>2</sub>O<sub>5</sub> was determined with a JEOL 8600 superprobe (EMPA) at the University of Saskatchewan, giving SiO<sub>2</sub> = 65.9 wt% and Na<sub>2</sub>O = 33.1 wt% (average of six microprobe spot analyses), corresponding to a formula of Na<sub>1.95</sub>Si<sub>2</sub>O<sub>5</sub>; the formula assumed for the X-ray structure analysis was Na<sub>2</sub>Si<sub>2</sub>O<sub>5</sub>. Other experimental details, pressure–temperature phase diagrams, and structure–composition relationships in the Na<sub>2</sub>O–SiO<sub>2</sub> system will be discussed elsewhere.

The product crystals were investigated by X-ray precession photography. Single-crystal measurements were made at room temperature and pressure with an Enraf–Nonius CAD-4F diffractometer and graphite-monochromatized MoK $\alpha$  X-radiation ( $\lambda = 0.70926 \text{ \AA}$ ). The crystal structure was solved with reflection data from a crystal of an earlier experiment at 4 GPa, 900°C (Experiment 1831; Ref. (8)) by Patterson synthesis with some assistance from direct methods. Structure refinements closely followed earlier procedures (16). Scattering factors for neutral atomic species and  $f'$ ,  $f''$  were taken from Ref. (17). All computations were carried out with DATAP77 and LINEX77 (State University of New York at Buffalo). Further experimental details for the refinement of the crystal from experiment 1919 are given below, and the results are summarized in Tables 1–4.<sup>1</sup>

Epsilon Na<sub>2</sub>Si<sub>2</sub>O<sub>5</sub> is orthorhombic with  $a = 5.580(1)$ ,  $b = 9.441(4)$ ,  $c = 8.356(3) \text{ \AA}$ ,  $V = 440.2 \text{ \AA}^3$ , space group  $Pbc2_1$  (No. 29),  $Z = 4$ , and  $D_x = 2.749 \text{ g} \cdot \text{cm}^{-3}$ . A total of 5134 reflections with indices  $\pm h, k, \pm l$  to  $2\theta = 80^\circ$  were measured in the  $\omega$  scan mode. Transmission factors varied from 0.890 for 100 to 0.920 for 160 (crystal volume =  $1.87 \times 10^{-3} \text{ mm}^3$ ,  $\mu = 9.27 \text{ cm}^{-1}$ ). There were 1426 unique

<sup>1</sup> See NAPS document No. 05235 for 12 pages of supplementary materials. Order from ASIS/NAPS, Microfiche Publications, P.O. Box 3513, Grand Central Station, New York, NY 10163-3513. Remit in advance \$4.00 for microfiche copy or for photocopy, \$7.75 up to 20 pages plus \$.30 for each additional page. All orders must be prepaid. Institutions and Organizations may order by purchase order. However, there is a billing and handling charge for this service of \$15. Foreign orders add \$4.50 for postage and handling, for the first 20 pages, and \$1.00 for additional 10 pages of material, \$1.50 for postage of any microfiche orders.

TABLE 1  
Positional and Isotropic Thermal Parameters ( $\text{\AA}^2$ )  $B_{eq} = \frac{1}{3} \sum_i \sum_j \beta_{ij} a_i \cdot a_j$

	<i>x</i>	<i>y</i>	<i>z</i>	$B_{eq}$
Na(1)	0.0616(3)	0.5113(2)	0.9775(3)	1.50(3)
Na(2)	0.0871(3)	0.2538(2)	0.2544(3)	1.47(3)
Si(1)	0.6296(2)	0.3080(1)	0.0570(2)	0.58(2)
Si(2)	0.5484(2)	0.0471(1)	0.2500	0.56(1)
O(1)	0.8902(5)	0.2668(3)	0.9996(5)	0.91(4)
O(2)	0.6422(5)	0.4202(3)	0.2084(4)	1.04(5)
O(3)	0.4601(5)	0.3858(3)	0.9202(4)	0.77(4)
O(4)	0.1816(5)	0.4998(3)	0.2482(6)	1.14(4)
O(5)	0.4735(5)	0.1710(3)	0.1200(4)	0.80(4)

reflections, with 318 considered unobserved on the basis of  $I < 3\sigma(I)$ . All reflections systematically absent in space group  $Pbc2_1$  had zero intensity using  $I < 3\sigma(I)$ . Refinement in  $Pbc2_1$  converged to  $R = 0.040$ ,  $R_w = 0.041$  [for reflections with  $I \geq 3\sigma(I)$ ,  $S = 1.690$ ,  $g = 0.06(2) \times 10^{-4}$ ,  $\Delta\rho = -1.13 \text{ e\AA}^{-3}$  at Si(2) to  $1.00 \text{ e\AA}^{-3}$  at Na(2)]. Because  $Pbc2_1$  is a polar space group, the *z* coordinate of Si(2) was arbitrarily fixed at 0.25, and therefore has no quoted e.s.d. in Table 1.

The crystal from experiment 1831 yielded unit-cell parameters [ $a = 5.568(5) \text{ \AA}$ ,  $b = 9.428(2) \text{ \AA}$ , and  $c = 8.349(5) \text{ \AA}$ ] similar to those for the crystal from experiment 1919 and the positional parameters were identical within error. However, the structure refinement was inferior ( $R = 0.089$  for isotropic thermal parameters) and is not presently reported.

TABLE 2  
Selected Bond Distances ( $\text{\AA}$ ) and Angles ( $^\circ$ )

Na(1)–O(1)	2.505(3)	Si(2)–O(2) <sup>I</sup>	1.639(2)
Na(1)–O(1)	2.434(3)	Si(2)–O(3)	1.633(3)
Na(1)–O(2)	2.864(3)	Si(2)–O(4) <sup>I</sup>	1.571(1)
Na(1)–O(3)	2.565(2)	Si(2)–O(5)	1.650(3)
Na(1)–O(4)	2.361(5)	⟨Si(2)–O⟩	1.623
Na(1)–O(4)	2.350(4)	O(1)–Si(1)–O(2)	110.6(2)
⟨Na(1)–O⟩	2.513	O(1)–Si(1)–O(3)	115.2(2)
Na(2)–O(1)	2.399(4)	O(1)–Si(1)–O(5)	113.0(2)
Na(2)–O(1)	2.333(3)	O(2)–Si(1)–O(3)	105.6(2)
Na(2)–O(3)	2.826(3)	O(2)–Si(1)–O(5)	106.4(2)
Na(2)–O(4)	2.383(3)	O(3)–Si(1)–O(5)	105.5(2)
Na(2)–O(4)	2.828(3)	O(2) <sup>I</sup> –Si(2)–O(3)	105.8(2)
Na(2)–O(5)	2.554(2)	O(2) <sup>I</sup> –Si(2)–O(4) <sup>I</sup>	114.4(2)
⟨Na(2)–O⟩	2.554	O(2) <sup>I</sup> –Si(2)–O(5)	102.4(2)
Si(1)–O(1)	1.580(1)	O(3)–Si(2)–O(4) <sup>I</sup>	114.1(2)
Si(1)–O(2)	1.652(3)	O(3)–Si(2)–O(5)	102.8(2)
Si(1)–O(3)	1.655(3)	O(4) <sup>I</sup> –Si(2)–O(5)	116.0(2)
Si(1)–O(5)	1.646(2)	Si(1)–O(2)–Si(2) <sup>I</sup>	127.1(2)
⟨Si(1)–O⟩	1.633	Si(1)–O(3)–Si(2) <sup>II</sup>	127.0(2)
		Si(1)–O(5)–Si(2)	129.3(2)

Note, (I)  $x, 1/2 + y, z$ . (II)  $x, 1/2 - y, 1/2 + z$ .

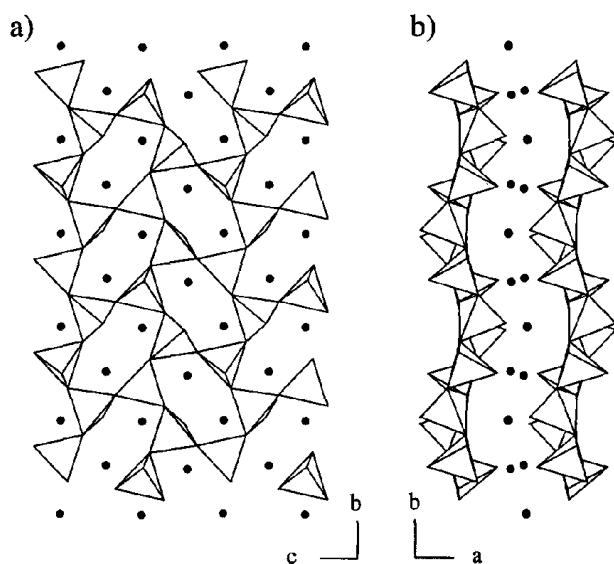


FIG. 1. Polyhedral representation of the  $[\text{Si}_2\text{O}_5]$  disilicate sheet structure of  $\epsilon\text{-Na}_2\text{Si}_2\text{O}_5$  with sodium represented by filled circles: (a)  $a$ -axis projection, showing alternating six-membered rings of UUUUDD and DDDDUU  $\text{SiO}_4$  tetrahedra; (b)  $c$ -axis projection, showing structural crenulation.

## DISCUSSION

The structure of  $\epsilon\text{-Na}_2\text{Si}_2\text{O}_5$  is based on a  $[\text{Si}_2\text{O}_5]$  disilicate sheet of alternating six-membered rings of UUUUDD and DDDDUU (where U is upward- and D downward-pointing)  $\text{SiO}_4$  tetrahedra in the (100) plane (Fig. 1a). The sheets have a gentle undulation in the  $c$ -axis projection (Fig. 1b), with a wavelength of two ring diameters defined by the  $b$  glide, but are essentially flat in the  $b$ -axis projection. The disilicate sheets are linked by two nonequivalent sodium cations that form short ( $\leq 2.5$  Å) bonds to the apical (nonbridging; nbr) oxygen atoms [O(1), O(4); Table 2, Fig. 2]. The bonding sphere for sodium is presently limited arbitrarily to 2.9 Å. Both bonds from silicon to nonbridging oxygen are very short (1.57–1.58 Å), as expected for silicates of low field strength cations, but these short  $\text{Si}-\text{O}_{\text{nbr}}$  bonds are compensated for by relatively long  $\text{Si}-\text{O}_{\text{br}}$  bonds (1.63–1.66 Å). Calculated bond valences (18) are: Na(1)—0.93; Na(2)—0.87; Si(1)—3.98; Si(2)—4.09; O(1)—1.87; O(2)—1.98; O(3)—2.12; O(4)—1.86; and O(5)—2.03. Bridging oxygens are either saturated or slightly overbonded and nonbridging oxygens are slightly underbonded, but the oxygen bond strength sum is 9.87, in good agreement with the ideal value of 10.0. An important feature of this structure is the relatively small  $\text{Si}-\text{O}-\text{Si}$  bond angles (127.0–129.3°; Table 2), that are significantly below the average of about 139° for all silicates and fall in the range of 124–137° for three-coordinated bridging oxygen in silicates (5).

Epsilon  $\text{Na}_2\text{Si}_2\text{O}_5$  has a perfect {100} cleavage which

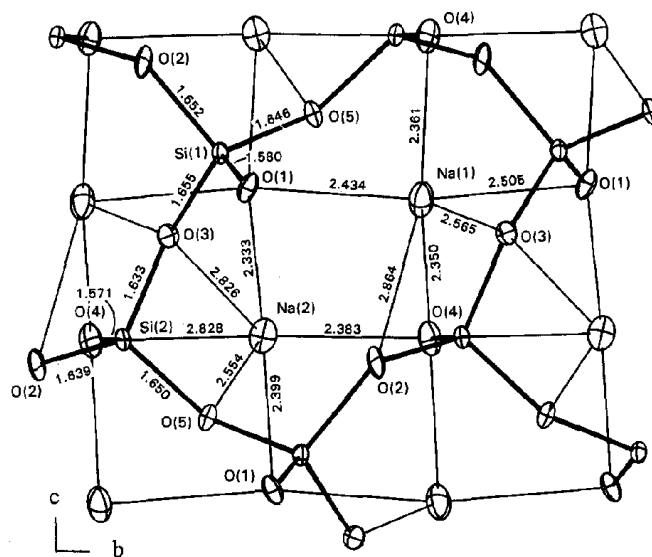


FIG. 2. Details of the stereochemistry of Si and Na in  $\epsilon\text{-Na}_2\text{Si}_2\text{O}_5$ :  $a$ -axis projection; bond distances are in Å.

combined with the manner of synthesis evidently resulted in deformation and degradation of the diffraction quality of single crystals. Interestingly, the partial slip deformation that developed during decompression of the high-pressure products is channeled along [001], as is evident in the preferred alignment of the major axes of thermal ellipsoids (Fig. 2) and the increase in  $R$  value for the structure refinement with an increase in the  $l$  Miller index (Fig. 3). Apparently, it is easier to slide the  $[\text{Si}_2\text{O}_5]$  disilicate sheets along the structural crenulation than across it (Fig. 1).

The minor discrepancies between the structure refine-

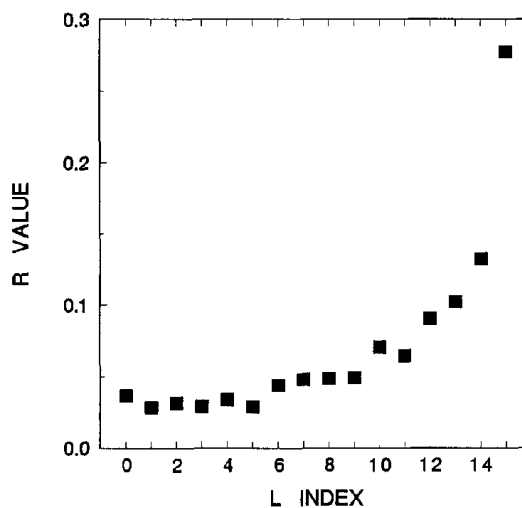


FIG. 3. Progressive increase in  $R$  value for the structure refinement of  $\epsilon\text{-Na}_2\text{Si}_2\text{O}_5$  with an increase in the  $l$  Miller index, related to the mosaic spread along the  $c$ -axis direction.

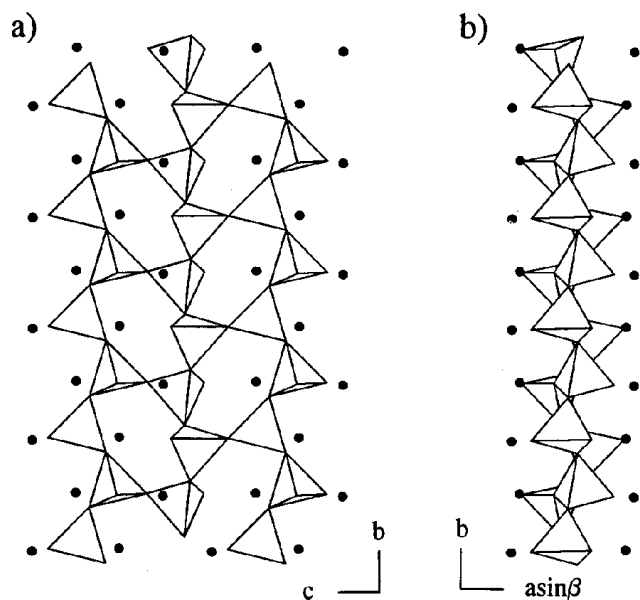


FIG. 4. Polyhedral representation of the  $[\text{Si}_2\text{O}_5]$  disilicate sheet structure of  $\beta\text{-Na}_2\text{Si}_2\text{O}_5$  with sodium represented by filled circles: (a)  $a$ -axis projection, showing six-membered rings of UDUDUD  $\text{SiO}_4$  tetrahedra; (b)  $c$ -axis projection.

ment presently reported and that for the second crystal prepared at 4 GPa and  $900^\circ\text{C}$  are attributable to the differential effects of decompression. A pressure-induced change in crystal structure was not observed.

The unit cell of  $\varepsilon\text{-Na}_2\text{Si}_2\text{O}_5$  was chosen to facilitate comparison with  $\beta\text{-Na}_2\text{Si}_2\text{O}_5$  (3, 4), and the two structures are indeed closely comparable (Figs. 1 and 4). The structure of the 1 bar,  $610\text{--}700^\circ\text{C}$  polymorph has six-membered rings of UDUDUD  $\text{SiO}_4$  tetrahedra. Although the  $[\text{Si}_2\text{O}_5]$  disilicate sheet is fairly flat, in detail it is slightly undulating in the  $c$ -axis projection (Fig. 4b) with a wavelength of one ring diameter. Accommodation of the sodium cations results in relative displacement of the  $[\text{Si}_2\text{O}_5]$  disilicate sheets along the  $c$ -axis, giving a monoclinic unit cell. The difference in the directedness within the six-membered rings of  $\varepsilon\text{-Na}_2\text{Si}_2\text{O}_5$  (UUUDDD and DDDDUU) and  $\beta\text{-Na}_2\text{Si}_2\text{O}_5$  (UDUDUD) is also mirrored in the difference in chain periodicity: vierer chains parallel to  $[010]$  and  $[001]$  in the  $\varepsilon$ -phase but zweier chains parallel to  $[010]$  and vierer chains parallel to  $[001]$  in the  $\beta$ -phase.

Densification in  $\varepsilon\text{-Na}_2\text{Si}_2\text{O}_5$  is accommodated largely by a decrease in dihedral ( $\text{Si—O—Si}$ ) bond angles to  $127.0^\circ\text{--}129.3^\circ$  ( $D_x = 2.75 \text{ g} \cdot \text{cm}^{-3}$ ; 7 GPa,  $1100^\circ\text{C}$ ), compared with  $135.1^\circ\text{--}137.1^\circ$  for  $\beta\text{-Na}_2\text{Si}_2\text{O}_5$  ( $D_x = 2.57 \text{ g} \cdot \text{cm}^{-3}$ ; 1 bar,  $610\text{--}700^\circ\text{C}$ ) and  $138.9^\circ\text{--}160.0^\circ$  for  $\alpha\text{-Na}_2\text{Si}_2\text{O}_5$  ( $D_x = 2.50 \text{ g} \cdot \text{cm}^{-3}$ ; 1 bar,  $> 700^\circ\text{C}$ ). The structure of  $\varepsilon\text{-Na}_2\text{Si}_2\text{O}_5$  supports our earlier suggestion (7) that densification of polymerized silicate melts to moderate pressures is accommodated predominantly by a decrease in dihedral bond angle

through crimping of  $\text{SiO}_4$  tetrahedral ring structures and a decrease in the number of  $\text{SiO}_4$  tetrahedra per ring (ring size). This suggestion is supported by the rather modest amounts of sixfold coordinated silicon ( $^{16}\text{Si}$ ) observed by  $^{29}\text{Si}$  MAS NMR and SiK-edge XANES spectroscopy in high-pressure alkali silicate glasses (9, 14). High-pressure melt structures probably consist of mixtures of collapsed and small-membered  $\text{SiO}_4$  rings and  $\text{SiO}_6$  octahedra, with the proportion of the latter increasing with an increase in pressure. The change from predominantly  $^{14}\text{Si}$  to predominantly  $^{16}\text{Si}$  should occur in alkali silicate melts at somewhat greater pressures than for crystalline phases because of the entropy factor. A predominant role for  $^{15}\text{Si}$  has yet to be demonstrated.

The X-ray structure of  $\varepsilon\text{-Na}_2\text{Si}_2\text{O}_5$  is consistent with a recent  $^{29}\text{Si}$  MAS NMR study (13) that showed two distinct peaks at  $-81.0$  and  $-82.3$  ppm (relative to TMS), and attributed them to silicate units with silicon in tetrahedral coordination. However, the Raman spectrum of  $\varepsilon\text{-Na}_2\text{Si}_2\text{O}_5$  reported in Ref. (13) was somewhat misleading. A strong Raman band at  $1076 \text{ cm}^{-1}$  did correctly indicate a  $Q^3$  (sheet) silicate structure, but the structure was interpreted to contain three-membered rings of  $\text{SiO}_4$  tetrahedra based on a strong band at  $643 \text{ cm}^{-1}$ . Evidently, the extreme crimping of the six-membered rings of  $\text{SiO}_4$  tetrahedra in  $\varepsilon\text{-Na}_2\text{Si}_2\text{O}_5$  results in a shift to higher wavenumbers of the low-frequency  $\text{Si—O—Si}$  symmetric stretching band from the value normally associated with disilicate units ( $550 \text{ cm}^{-1}$  (19) to  $643 \text{ cm}^{-1}$ ). We had previously associated a prominent Raman band at  $\approx 600 \text{ cm}^{-1}$  in the spectra of silicate glasses with three-membered ring structures (20), but recognized that the shift of this feature to higher wavenumbers actually represents a progressive change in intermediate-range structure associated with progressive closing of the  $\text{Si—O—Si}$  bond angle.

#### ACKNOWLEDGMENTS

We thank two unnamed reviewers for helpful comments, Y. Thibault and R. W. Luth for running the high-pressure experiment, Y. Pan for EMPA, and the Natural Sciences and Engineering Research Council of Canada for financial support.

#### REFERENCES

1. J. Williamson and F. P. Glasser, *Phys. Chem. Glasses* **7**, 127 (1966).
2. A. K. Pant and D. W. J. Cruickshank, *Acta Crystallogr. Sect. B* **24**, 13 (1968).
3. F. Liebau, *Acta Crystallogr.* **14**, 395 (1961).
4. A. K. Pant, *Acta Crystallogr. Sect. B* **24**, 1077 (1968).
5. F. Liebau, "Structural Chemistry of Silicates." Springer-Verlag, Berlin, 1985.
6. E. Ito and T. Takahashi, in "High-Pressure Research in Mineral Physics" (M. H. Manghnani and Y. Syono Eds.), AGU Geophysical Monograph, Vol. 39, p. 221 (1987).
7. G. S. Henderson and M. E. Fleet, *Trans. Am. Crystallogr. Assoc.* **27**, 269 (1991).

8. M. E. Fleet and G. S. Henderson, *EOS Trans. AGU* **75**, 370 (1994).
9. X. Xue, J. F. Stebbins, M. Kanzaki, P. F. McMillan, and B. Poe, *Am. Mineral.* **76**, 8 (1991).
10. X. Xue, J. F. Stebbins, and M. Kanzaki, *Am. Mineral.* **79**, 31 (1994).
11. L. W. Finger and R. M. Hazen, *Acta Crystallogr. Sect. B* **47**, 561 (1991).
12. M. Kanzaki, X. Xue, and J. F. Stebbins, *EOS Trans. AGU* **70**, 1418 (1989).
13. B. D. Santarsiero, X. Xue, and M. Kanzaki, *Trans. Am. Crystallogr. Assoc.* **27**, 279 (1991).
14. D. Li, M. E. Fleet, G. M. Bancroft, M. Kasrai, and G. S. Henderson, *EOS Trans. AGU* **75**, 370 (1994).
15. M. E. Fleet and G. S. Henderson, *Phys. Chem. Mineral.*, in press.
16. M. E. Fleet, *Am. Mineral.* **77**, 76 (1992).
17. J. A. Ibers and W. C. Hamilton, Eds., "International Tables for X-Ray Crystallography," Vol. IV. Kynoch Press, Birmingham, UK, 1974.
18. I. D. Brown, in "Structure and Bonding in Crystals" (M. O'Keeffe and A. Navrotsky Eds.), p. 1. Academic Press, New York, 1981.
19. P. McMillan, *Am. Mineral.* **69**, 622 (1984).
20. G. S. Henderson, G. M. Bancroft, M. E. Fleet, and D. J. Rodgers, *Am. Mineral.* **70**, 946 (1985).